Analytical Methods

ROYAL SOCIETY OF CHEMISTRY

PAPER

View Article Online
View Journal | View Issue

Cite this: *Anal. Methods*, 2024, **16**, 6049

Single reaction chamber microwave digestion coupled with ICP-MS for the determination of ultra-trace mercury in rocks

Minsi Liang * and Hongtao Liu*

Received 5th May 2024
Accepted 7th August 2024

DOI: 10.1039/d4ay00824c

rsc.li/methods

In this study, a method for rock digestion using a single reaction chamber (SRC) microwave system was established. Nitric acid (HNO_3) and hydrofluoric acid (HF) were used as digestion agents, and the determination of mercury (Hg) in rocks was performed by inductively coupled plasma mass spectrometry (ICP-MS). The optimal conditions for the SRC microwave system were achieved at 260 °C and 70 bar, with a mixture of 3 mL of 65–68 wt% HNO_3 and 1 mL of 49 wt% HF when the sample weight is in the range of 0.025–0.05 g. The method quantitation limit (MQL) was determined to be 0.0016 mg kg^{-1}. Measurement accuracy was evaluated using five Chinese nationally certified reference materials, demonstrating good consistency between measurement results and certified values. The method was applied to two rock samples, resulting in a recovery rate ranging from 105% to 109%. This method exhibits high sensitivity, stability, and low acid consumption. Importantly, it provides a reliable and efficient determination method for Hg in rocks, which is of great significance in geochemical analysis.

Introduction

Mercury (Hg) is a naturally occurring element in the Earth's crust. It is a heavy, silvery metal that is liquid at room temperature. Mercury is highly toxic to humans and animals. Hg in the environment can come from both natural sources and human activities. Natural sources include volcanic eruptions, the weathering of rocks, and forest fires, which release mercury into the atmosphere. Human activities, such as industrial processes, coal combustion, and mining, also contribute to the release of mercury into the environment. Additionally, the improper disposal of products containing mercury, such as fluorescent light bulbs and thermometers, can lead to mercury contamination in soil and water.[1] Hg plays a significant role in geochemical research, particularly in theoretical geochemistry, exploration geochemistry, and ecological and environmental geochemical assessment. It is an important element for evaluating the geochemistry of the Earth. In geochemical assessments, the abundance of mercury in the Earth's crust, rocks, and sediment is commonly used as a measure. Therefore, the determination of Hg in these geological materials holds great significance. This includes the challenging task of measuring mercury in rocks, which is a crucial aspect of geochemical research.

Rocks often contain minerals with high resistance to chemical erosion, making it challenging to achieve complete dissolution of the sample. Certain minerals, such as silicates and oxides, may require harsh digestion conditions to break down effectively. In addition, Hg, which is present in these rocks at relatively low concentrations with an average level of μg kg^{-1}, is known to be volatile, and high temperatures during the digestion process can lead to significant losses of Hg. This volatility of Hg poses an additional challenge in obtaining accurate Hg concentration measurements from the rock samples.

To accurately detect Hg at such low concentrations in the rocks, highly sensitive analytical techniques are required, such as inductively coupled plasma optical emission spectrometry (ICP-OES),[2–8] inductively coupled plasma mass spectrometry (ICP-MS),[9–13] atomic fluorescence spectrometry (AFS),[14–17] cold vapor atomic absorption spectrometry (CVAAS),[18] direct mercury analyzer (DMA),[19] *etc.* ICP-MS can detect trace levels of elements at concentrations as low as parts per trillion, making it an extremely sensitive technique for elemental analysis. Moreover, it has low background noise, which allows for accurate and precise measurements of trace elements in samples with a complex matrix, thus suitable for the accurate determination of Hg at the μg kg^{-1} level.[20–22] The disadvantages of AFS include higher reagent consumption, potential for introducing pollution, and lower efficiency. On the other hand, CVAAS exhibits lower sensitivity, necessitating intricate steps such as separation and enrichment.[23,24]

While the literature is sparse regarding the precise determination of mercury in rock samples, we have identified two studies that offer relevant comparisons. One study, reported in the literature, employs a direct mercury analyzer for the quantitative determination of mercury in silicate rocks, with

Instrumental Analysis & Research Center, Sun Yat-Sen University, Guangzhou 510275, P. R. China. E-mail: liangmsi@mail.sysu.edu.cn

detection and quantification limits of 1.3 ng and 3.0 ng, respectively.[18] These figures are notably higher by two orders of magnitude than the limits achievable with ICP-MS, indicating the superior sensitivity of our approach. Another study employs a solid sampling-cold atomic absorption method for mercury determination in rock minerals. Although its detection limit is comparable to that of ICP-MS, this method requires several enrichment steps to attain such sensitivity, which contrasts with the efficiency of ICP-MS which does not necessitate such extensive sample preparation.[24]

ICP-MS is widely used for elemental analysis of geological samples.[25–28] The sample preparation method for ICP-MS analysis of rocks typically involves a digestion process to dissolve the solid rock matrix, normally involving the use of strong acids, such as nitric acid (HNO_3) or hydrofluoric acid (HF), to decompose the rocks and solubilize the Hg into a liquid solution. Conventional heating wet digestion and microwave digestion are two common methods for sample preparation. Mercury has a high propensity to vaporize, especially when exposed to heat and strong acids, which would cause the loss of Hg during the wet digestion procedure for open vessels and lead to lower concentration results than expected in the final solution. The conventional microwave digestion method, which involves digesting samples in a high-pressure closed state, can reduce the loss of mercury in rock samples. However, if the digestion temperature is too high, it can also cause mercury loss. One study indicates that when determining mercury in soil using the microwave digestion-ICP-MS method, the element's volatility can lead to significant losses if the digestion temperature is too high or the holding time is excessively long. Therefore, it is recommended to keep the digestion temperature below 180 °C to mitigate mercury loss.[29] The other study has reported that even when using ICP-MS in conjunction with closed-vessel microwave digestion to determine mercury content in coal, mercury losses can still occur when the digestion temperature is controlled at 240 °C.[30]

The technology of a single reaction chamber (SRC) system with microwave heating became commercially available. It utilizes a single reaction chamber with a closed space that is pressurized with an inert gas, such as nitrogen, to reach supercritical conditions. It allows a maximum temperature and pressure of 300 °C and 200 bar, which can solve the problem of digesting the most difficult samples in the laboratory. In this regard, the SRC microwave system has been used at high temperatures and pressures to decompose organic matrices such as carbohydrate-rich foods,[31] milk powder,[32,33] active pharmaceutical ingredients,[34] rice,[35] fuel oils,[36,37] *etc.* Moreover, the boiling point of all the matter will increase dramatically under ultra-high pressure. Thus, the use of ultra-high pressure during the digestion procedure could reduce the risk of losses for the volatile elements, especially for Hg.[38–40] According to the Clausius–Clapeyron equation, the boiling point of Hg under 200 bar is calculated to be 909.123 °C, much higher than the one under standard pressure (356.619 °C). As a result, by using the pre-pressurization technology, the digestion solution does not boil, and the loss of Hg will reduce dramatically even at high temperatures. Overall, the SRC microwave system represents a cutting-edge technology that offers significant improvements in terms of speed, efficiency, and reliability for the digestion of solid samples in preparation for elemental analysis.

In our specific methodology, prior to this study, we initially experimented with a conventional microwave digestion system for the digestion of rock samples. However, we faced difficulties in achieving complete digestion with this method. The rock matrix's complexity, characterized by its high mineral content and varying hardness levels, posed a challenge in ensuring uniform and thorough digestion following standard microwave digestion protocols. These preliminary experiments with the conventional system highlighted the need for an alternative approach.

As a result, we explored and ultimately selected a different digestion method that proved more effective in decomposing the rock samples and liberating mercury for analysis. In this work, we evaluated the SRC microwave system for rock digestion, utilizing HNO_3 and HF as digestion agents for mercury determination by ICP-MS techniques. To enhance the digestion efficiency, we investigated various parameters including digestion temperature, pre-pressurization, and the volume of digestion agents in the rock digests. Through this process, we established a fast, sensitive, and stable method for detecting mercury content in rocks.

Experimental

Instruments

An ICP-MS (iCAP Qc, Thermo Fisher, Germany) equipped with a polyfluoroalkoxy (PFA) concentric pneumatic nebulizer and a PFA cyclonic spray chamber, was used for all measurements of Hg in rocks. The formation of the Au complex reduces the memory effect of mercury and maintains the stability of mercury by adding Au + solution into the standard solution as well as the sample solution. The selection of internal standard element Ir can effectively avoid non-mass spectrum interference. Selecting isotope ^{202}Hg for quantification and kinetic energy discrimination mode (KED) was used to reduce mass spectrum interference. The operational parameters are listed in Table 1. A SRC microwave system (Ultra WAVE, Milestone, Italy) equipped with 40-position 15 mL Teflon digestion tubes has been utilized at high temperatures and pressures to decompose rock samples. The operational parameters are listed in Table 2. An electronic analytical balance (XP6, Mettler-Toledo, Switzerland) was used for weighing the samples. An ultrapure water system (Milli-Q Advantage A10, Millipore, France) was used for deionized water (18.2 MΩ cm) preparation. An acid purification system (SubCLEAN, Milestone, Italy) was used for guaranteed reagent (HNO_3) further purification.

Reagents, standard solutions, and samples

Deionized water was used in all experiments. Nitric acid (GR, 65–68 wt%) and hydrofluoric acid (GR, 49 wt%) were supplied by Guangzhou Chemical Reagent Co., Ltd (Guangzhou, China).

Stock standard solutions of Hg, Au and Ir (1000 mg L^{-1}) were supplied by the National Analysis and Testing Center for

Table 1 Optimized instrumental parameters for ICP-MS

Items	Values/status
Plasma RF power	1550 W
Nebulizer gas flow (Ar)	0.83 L min^{-1}
Auxiliary gas flow (Ar)	0.8 L min^{-1}
Cool gas flow (Ar)	14 L min^{-1}
Sampling depth	5 mm
Collision gas flow (He)	4.53 mL min^{-1}

Nonferrous Metals and Electronic Materials (Beijing, China). Stock standard solutions of Hg were used for the preparation of seven concentration levels (0.01, 0.02, 0.05, 0.1, 0.2, and 0.5 μg L^{-1}), which were used for establishing calibration curves. Calibration solutions were freshly prepared by dilution of stock standard solution with 2% HNO_3 at suitable concentrations for different analytical methods.

The standard stock solution of Ir was used for the preparation of 10 μg L^{-1} internal standard solution because Ir is extraordinarily low in rocks. To avoid the Hg memory effect, 100 μg L^{-1} standard solution of Au was added to maintain the stability of mercury in the standard solution of Hg and samples.

Certified reference materials for the chemical composition of rocks including granite GSR-1 (GBW07103), quartz sandstone GSR-4 (GBW07106), granodiorite GSR-9 (GBW07111), andesite GSR-8 (GBW07110) and granitic gneiss GSR-14 (GBW07121) were from the Institute of Geophysical and Geochemical Exploration, Chinese Academy of Geological Sciences (Langfang, China).

Rock sample 1 and rock sample 2 were from the South China Sea Institute of Oceanology.

Sample digestion[41]

Taking into consideration the volatile behavior of Hg in rocks, the samples were digested using a SRC microwave system. About 0.025 g–0.05 g of the sample (n = 3/6) was placed in a 15 mL Teflon digestion tube, and HNO_3–HF mixtures (3 mL of 65–68 wt% HNO_3 and 1 mL of 49 wt% HF) were added to the tube, following the SRC microwave system digestion procedure (Table 2).

After digestion, the digested samples were transferred to PFA (polyfluoroalkoxy) volumetric flasks (resistant to HF corrosion) without being subjected to drying on an electric hot plate to avoid the volatile loss of Hg and then were diluted with deionized water to 10 mL for ICP-MS analysis. The same procedure was applied to all samples. Blank solutions were also prepared as above.

Measurement using ICP-MS

A meticulous pre-conditioning protocol was implemented for the ICP-MS spectrometer to guarantee its operational stability and reproducibility. Prior to each analytical session, a mandatory period of at least 30 minutes was dedicated to a comprehensive pre-treatment regimen. This process encompassed thorough cleaning of the system components and subsequent equilibration, aimed at mitigating potential matrix effects and memory effects inherent to the analysis of samples containing high acid concentrations. By adopting this rigorous pre-conditioning approach, we aimed to minimize any confounding factors that could adversely affect the accuracy and precision of our ICP-MS measurements.

Torch position and ion lenses were first optimized. The operating conditions (torch position, lenses, gas flows and detector voltage) were optimized daily in normal-, and high-resolution modes, and then the instrumental parameters were optimized in the CCT mode to maximize ion signals, using iCAP Q TUNE aqueous multi-element standard solution in 2% HNO_3 and 0.5% HCl solution (Thermo Scientific).

Each solution was measured 6 times and the quantification of Hg was carried out using external calibration curves. The correlation coefficients (r) for all the calibration curves were at least 0.9997, reflecting a good linear relationship throughout the ranges of concentrations under study. We used the most abundant isotope of ^{202}Hg for quantification and online added Ir as an internal standard. Between sample measurements, the sample introduction system was rinsed with 2% HNO_3 for 1–2 min.

Results and discussion

Optimization of the SRC microwave digestion procedure

The classification of rocks primarily encompasses three major categories: igneous rocks, sedimentary rocks, and metamorphic rocks. In this experiment, the digestion conditions were optimized using standard samples of these three categories: granite GSR-1 (GBW07103), quartz sandstone GSR-4 (GBW07106) and granodiorite GSR-9 (GBW07111). The pre-pressure, maximum microwave temperature and holding time were optimized (Table 3). The maximum microwave temperature and the holding time mentioned here both refer to those optimized specifically for the third step of the microwave digestion program. After the completion of the microwave program for sample digestion, we observed two phenomena. One was incomplete digestion with solid residues in the solution, and the other was complete digestion resulting in a clear, colorless solution.

Based on the results, it is evident that the digestion of the rocks is influenced by the pre-pressure, digestion temperature,

Table 2 Microwave program for sample digestion

Program	Heating time (min)	Temperature (°C)	Holding time (min)	The limit pressure (bar)	External wall protection temperature (°C)
1	10	90	5	100	60
2	10	160	5	130	60
3	15	260	30	180	60

Table 3 Effect of SRC microwave digestion conditions on the digestion effect of rocks

			Rocks					
			Granite GSR-1 (GBW07103)		Quartz sandstone GSR-4 (GBW07106)		Granodiorite GSR-9 (GBW07111)	
Pre-pressure (bar)	Temperature (°C)	Holding time (min)	Phenomena	Recovery of Hg (%)	Phenomena	Recovery of Hg (%)	Phenomena	Recovery of Hg (%)
30	240	30	Incomplete digestion	74	Incomplete digestion	78	Incomplete digestion	76
50	240	30	Incomplete digestion	83	Incomplete digestion	86	Incomplete digestion	77
50	240	60	Incomplete digestion	92	Incomplete digestion	87	Incomplete digestion	79
50	260	30	Complete digestion	98	Incomplete digestion	90	Incomplete digestion	86
70	240	30	Complete digestion	98	Incomplete digestion	92	Incomplete digestion	91
70	240	60	Complete digestion	105	Incomplete digestion	92	Incomplete digestion	93
70	260	30	Complete digestion	105	Complete digestion	98	Complete digestion	99
70	260	60	Complete digestion	109	Complete digestion	98	Complete digestion	101

and holding time. As the pre-pressure increases, higher digestion temperature and longer holding time, the digestion completeness increases. To optimize the digestion process and save time, we have selected SRC microwave digestion conditions of 70 bar of pre-pressure, a maximum temperature of 260 °C, and a holding time of 30 minutes for the test. The optimum digestion program is shown in Fig. 1. This condition is expected to provide efficient and complete digestion of the rocks while reducing the overall digestion time.

Digestion reagents

Rocks typically contain various minerals and oxides. In this case, the use of a HNO_3–HF system is common as a digestion solution. Through testing, it has been found that for rock samples in the range of 0.025 g to 0.05 g, the addition of 3 mL of HNO_3 and 1 mL of HF as the digestion system is sufficient to completely dissolve the sample. This combination of acids is effective in decomposing the various components of the rocks, releasing Hg for accurate analysis.

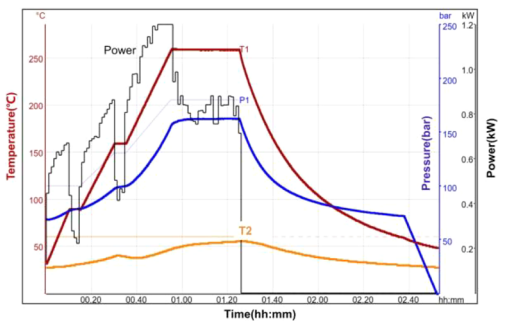

Fig. 1 Running profile (power, temperature, and pressure) for a SRC microwave digestion. Power represents the behaviour of microwave power, T1 represents the behaviour of the internal temperature of the pressure vessel, P1 represents the behaviour of the internal pressure of the pressure vessel, and T2 represents the behaviour of the vessel external wall temperature.

Detection limits and quantitation limits[36]

Table 4 provides information on the linear range of the calibration curve, the regression equation used to fit the data, the correlation coefficient (r) indicating the strength of the linear relationship, and the instrument detection limit (IDL), the instrument quantitation limit (IQL), the method detection limit (MDL), and the method quantitation limit (MQL) for Hg. The MDL and MQL values are based on a sample weight of 0.05 g and a sample preparation volume of 10 mL. The table shows that the Hg demonstrates a strong linear relationship with the corresponding signal intensity within the range of 0 to 0.5 μg L^{-1}, with a high correlation coefficient of 0.9999. The IDL and IQL values indicate the sensitivity and accuracy of the instrument in detecting and quantifying low concentrations of Hg, while the MDL and MQL values provide information on the method's detection and quantitation limits for Hg in real samples.

Evaluation of uncertainty

To determine the accuracy of the measurement method, we measured five certified reference materials and evaluated the uncertainty of the measurement method.[42] The E_n value method was used to assess the agreement between the measurement results and the certified values.[43]

Establishment of the measurement model

Based on the measurement method, a measurement model of a linear function was established. Eqn (1) is employed as the

Table 4 The calibration curve, correlation coefficient (r), detection limits and quantitation limits

Linear range (μg L^{-1})	Regression equation	Correlation coefficient (r)	IDL (μg L^{-1})	IQL (μg L^{-1})	MDL (mg kg^{-1})	MQL (mg kg^{-1})
0–0.5	$y = 21\,734.632x + 71.813$	0.9999	0.0025	0.0084	0.0005	0.0016

measurement model for uncertainty evaluation during the measurement process of Hg in rocks.

$$W = \frac{C \times V}{m \times 1000} \quad (1)$$

where W represents the element content in the sample, in mg kg^{-1}; C represents the concentration of the element in the sample solution, in μg L^{-1}; V represents the final volume of the sample after dilution, in mL; and m represents the mass of the sample, in g. From the mathematical model, the sensitivity coefficient for each component is 1.

Analysis of the uncertainty sources

Based on the mathematical model, the uncertainty components primarily consist of the following parameters:

(1) Uncertainty from linear fitting of the calibration curve ($u_{rel}(C)$).

(2) Uncertainty from sample preparation (u_{rel}(pre)).

(3) Uncertainty from random effects ($u_{rel}(C_{Rep})$).

The measurement uncertainty of Hg in rocks arises from the combination of uncertainties in each of the aforementioned parameters. The relative standard uncertainty ($u_{rel}(C_{all})$) is calculated using eqn (2):

$$u_{rel}(C_{all}) = \sqrt{u_{rel}(C)^2 + u_{rel}(\text{pre})^2 + u_{rel}(C_{Rep})^2} \quad (2)$$

Evaluation of uncertainty in linear fitting of the calibration curve

The standard uncertainty and relative standard uncertainty arising from the calibration of the standard curve using the least squares method to determine C are calculated using eqn (3)–(7).

$$C_{ave} = \frac{\sum_{i=1}^{n} C_i}{n} \quad (3)$$

$$S(y) = \sqrt{\frac{\sum_{i=1}^{n} [y_i - (a + bC_i)]^2}{n-2}} \quad (4)$$

$$S_{CC} = \sum_{i=1}^{n} (C_i - C_{ave})^2 \quad (5)$$

$$u(C) = \frac{S(y)}{b} \cdot \sqrt{\frac{1}{p} + \frac{1}{n} + \frac{(C - C_{ave})^2}{S_{CC}}} \quad (6)$$

$$u_{rel}(C) = \frac{u(C)}{C} \times 100\% \quad (7)$$

where C_{ave} represents the average concentration of the standard solutions, in μg L^{-1}; C_i represents the concentration of the series of standard solutions, in μg L^{-1}; n represents the number of measurements for the standard solutions; $S(y)$ represents the standard deviation of the residuals for the mass spectrometric peak response values of the standard solutions; y_i represents the intensity response value corresponding to C_i; a represents the intercept of the standard curve; b represents the slope of the standard curve; S_{CC} represents the sum of squared residuals for the mass concentrations of the standard solutions; C represents the average concentration of the element in the sample solutions, in μg L^{-1}; p represents the number of sample tests; $u(C)$ represents the standard uncertainty arising from the calibration of the sample solution's average concentration C using the least squares method for fitting the standard curve, in μg L^{-1}; and $u_{rel}(C)$ represents the relative standard uncertainty arising from the calibration of the sample solution's average concentration C using the least squares method for fitting the standard curve, expressed as a percentage.

The uncertainty introduced by fitting the standard curve using the least squares method for the samples was calculated, and the results are presented in Table 5.

Evaluation of uncertainty in sample preparation

The uncertainty in sample preparation arises primarily from the uncertainties in sample weighing and the final diluted volume. The balance used for sample weighing has been calibrated by the Guangdong Provincial Institute of Metrology. The calibration certificate specifies an expanded uncertainty of 3 μg for weighing samples in the range of 0.001 to 0.05 g. Therefore, the relative standard uncertainty ($u_{rel}(m)$) of samples ranging from 0.025 to 0.05 g is between 0.001% and 0.002%.

Table 5 Calculation results for uncertainty introduced by least squares fitting of the standard

	W (mg kg^{-1})										
Rocks	1	2	3	4	5	6	Average	p	SD	$u(C_{Rep})$ (mg kg^{-1})	$u_{rel}(C_{Rep})$ (%)
GSR-1 (GBW07103)	0.0045	0.0040	0.0043	0.0045	0.0043	0.0045	0.0044	6	0.0002	0.0001	2.3
GSR-4 (GBW07106)	0.0052	0.0059	0.0056	0.0057	0.0052	0.0056	0.0055	6	0.0003	0.0001	1.8
GSR-9 (GBW07111)	0.0352	0.0341	0.0342	0.0345	0.0350	0.0355	0.0348	6	0.0006	0.0002	0.58
GSR-8 (GBW07110)	0.0146	0.0134	0.0134	—	—	—	0.0138	3	0.0007	0.0004	2.9
GSR-14 (GBW07121)	0.0038	0.0036	0.0038	—	—	—	0.0037	3	0.0001	0.0001	2.7

The sample was finally diluted to 10 mL using a 10 mL volumetric flask. $E_{cal,i}$ represents the allowable error specified in the volumetric flask verification regulations, which is 0.02 mL. The relative standard uncertainty introduced by this process, $u_{rel}(V_i)$, is calculated using eqn (8) and (9).

$$u(V_i) = \frac{E_{cal,i}}{\sqrt{3}} \quad (8)$$

$$u_{rel}(V_i) = \frac{u(V_i)}{V_{o,i}} \quad (9)$$

where $u(V_i)$ represents the standard uncertainty introduced by the volumetric flask (i) during the volume determination, in mL; $E_{cal,i}$ represents the tolerance specified in the verification procedure for the volumetric flask, in mL; $u_{rel}(V_i)$ represents the relative standard uncertainty introduced by the volumetric flask during the volume determination, $V_{o,i}$ represents the nominal volume of the volumetric flask, in mL.

The result of the calculation is 0.12%. The total relative standard uncertainty introduced by sample preparation, u_{rel}(pre), is calculated using eqn (10), and the result of the calculation is 0.12%.

$$u_{rel}(\text{pre}) = \sqrt{u_{rel}(m)^2 + u_{rel}(V)^2} \quad (10)$$

Evaluation of uncertainty due to random effects

The value of W was calculated according to eqn (1). The uncertainty due to random effects from p measurements was determined using eqn (11) and (12). The results are presented in Table 6.

$$u(C_{Rep}) = \frac{SD}{\sqrt{p}} \quad (11)$$

$$u_{rel}(C_{Rep}) = \frac{u(C_{Rep})}{W} \quad (12)$$

where SD represents the standard deviation from p measurements, in mg kg^{-1}; $u(C_{Rep})$ represents the standard uncertainty introduced by random effects, in mg kg^{-1}; and $u_{rel}(C_{Rep})$ represents the relative standard uncertainty introduced by random effects, expressed as a percentage.

Calculation and representation of relative combined standard uncertainty and expanded uncertainty

The relative combined standard uncertainty, $u_{rel}(C_{all})$, is calculated using eqn (2) and the results are presented in Table 7. A graphical representation of the proportion of each uncertainty component is shown in Fig. 2. The results indicate that the uncertainty from sample preparation is relatively low.

At a coverage probability of 95%, with $k = 2$, the relative expanded uncertainty, U_{rel}, and the expanded uncertainty, U, are calculated using eqn (13) and (14), respectively. The calculation results are presented in Table 8. An E_n value evaluation is performed on the sample results, and all E_n values are less than 1, indicating satisfactory accuracy of the test results.

$$U_{rel} = k \cdot u_{rel}(C_{all}) \quad (13)$$

$$U = U_{rel} \cdot W \quad (14)$$

The recoveries of rock samples

The spiked recovery experiment was done during the digestion step. The recoveries of rock samples were determined in triplicate (Table 9). The original values ranged from 0.015 to 0.178 mg L^{-1}, and the spiked values were 0.01 and 0.05 mg L^{-1}, respectively. The recovery percentages were between 105% and 109%, with an average recovery of approximately 107%. The

Table 7 Calculation results of relative combined standard uncertainty

Rocks	$u_{rel}(C)$ (%)	u_{rel}(pre) (%)	$u_{rel}(C_{Rep})$ (%)	$u_{rel}(C_{all})$ (%)
GSR-1(GBW07103)	5.8	0.12	2.3	6.7
GSR-4(GBW07106)	4.7	0.12	1.8	5.6
GSR-9(GBW07111)	0.37	0.12	0.58	2.6
GSR-8(GBW07110)	0.35	0.12	2.9	3.8
GSR-14(GBW07121)	7.0	0.12	2.7	7.9

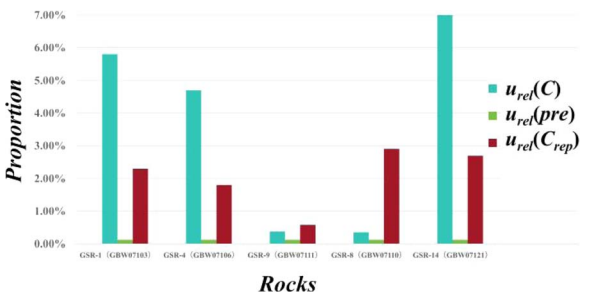

Fig. 2 Proportion of components in relative combined standard uncertainty.

Table 6 Uncertainty due to random effects

Rocks	n	p	C (μg L^{-1})	C_{ave} (μg L^{-1})	$S(y)$	S_{CC}	$u(C)$ (μg L^{-1})	$u_{rel}(C)$ (%)
GSR-1(GBW07103)	8	6	0.012	0.1106	28.33	0.2051	0.0007	5.8
GSR-4(GBW07106)	8	6	0.015				0.0007	4.7
GSR-9(GBW07111)	8	6	0.162				0.0006	0.37
GSR-8(GBW07110)	8	3	0.171				0.0006	0.35
GSR-14(GBW07121)	8	3	0.010				0.0007	7.0

Table 8 Representation of relative combined standard uncertainty, expanded uncertainty, and E_n value evaluation

Rocks	U_{rel} (%)	U (mg kg^{-1})	W (mg kg^{-1})	Representation of the measurement result (mg kg^{-1})	Certified value (mg kg^{-1})	E_n
GSR-1(GBW07103)	12.5	0.0005	0.0044	0.0044 ± 0.0005	0.0041 ± 0.0012	0.2
GSR-4(GBW07106)	10.0	0.0006	0.0055	0.006 ± 0.001	0.006 ± 0.002	0
GSR-9(GBW07111)	1.4	0.0005	0.0348	0.035 ± 0.001	0.035 ± 0.001	0
GSR-8(GBW07110)	5.8	0.0008	0.0138	0.014 ± 0.001	0.014 ± 0.003	0
GSR-14(GBW07121)	15.0	0.0006	0.0037	0.0037 ± 0.0006	0.0035 ± 0.0016	0.1

Table 9 The recoveries of rock samples ($p = 3$)

Samples	Original value (mg L^{-1})	Spiked value (mg L^{-1})	Measured value after spiking (mg L^{-1})	Recovery (%)	The average recovery (%)	RSD (%)
Rock sample 1	0.015	0.01	0.026	105	107	1.9
	0.016	0.01	0.027	109		
	0.015	0.01	0.026	108		
Rock sample 2	0.172	0.05	0.225	107	107	1.0
	0.172	0.05	0.225	106		
	0.178	0.05	0.232	108		

RSD of recovery was also calculated for each sample, indicating the precision of the method. The results indicate that the method is suitable for the recovery of rock samples with good accuracy and reproducibility.

Conclusions

In this study, a new method for the determination of ultra-trace Hg in rocks by ICP-MS combined with the digestion process of a SRC microwave system was proposed. The SRC system, equipped with microwave heating technology, solves the problem of digesting the most challenging rock samples in the laboratory. The pre-pressurization technology ensures that the digestion solution does not boil at high temperatures and pressure, thereby preventing the loss of Hg through vaporization. Based on this discovery, a quantitative method of Hg by ICP-MS was established, which utilized a correction coefficient of a standard solution. The method achieved a MQL of 0.0016 mg kg^{-1}. To determine the accuracy of the measurement method, five Chinese nationally certified reference materials were measured, and the uncertainty of the measurement method was evaluated. The E_n value method was employed to assess the agreement between the measurement results and the certified values, demonstrating good consistency. The method was applied to analyze two rock samples for ultra-trace Hg, and the recovery percentages ranged from 105% to 109%. This indicates that the method is both stable and reliable. Furthermore, the method offers a practical approach for accurately determining ultra-trace Hg in rocks.

Data availability

The original contributions presented in the study are included in the article; further inquiries can be directed to the corresponding authors.

Author contributions

Minsi Liang: conceptualization, data curation, formal analysis, resources, investigation, methodology, visualization, writing – original draft preparation. Hongtao Liu: resources, writing – reviewing and editing.

Conflicts of interest

There are no conflicts to declare.

References

1 K. G. Pavithra, P. SundarRajan, P. S. Kumar and G. Rangasamy, *Chemosphere*, 2023, **312**, 137314.
2 H. Ahmad, B. H. Koo and R. A. Khan, *Microchem. J.*, 2022, **175**, 107179.
3 Z. Cai and Z. Wang, *Anal. Chim. Acta*, 2022, **1203**, 339724.
4 K. Greda, M. Welna, A. Szymczycha-Madeja and P. Pohl, *Talanta*, 2022, **249**, 123694.
5 S. J. Abellán-Martín, J. Pérez, F. C. Pinheiro, J. A. Nóbrega, M. Á. Aguirre, L. Vidal and A. Canals, *Adv. Sample Prep.*, 2023, **7**, 100084.
6 Z. Yan, S. Yang and Z. Zhou, *World Nonferrous Metals*, 2021, **2**, 127–128.
7 J. Wang, M. Hao, J. Li, X. Wang and Y. Liu, *Metall. Anal.*, 2023, **43**, 74–78.
8 F. C. Pinheiro, M. Á. Aguirre, J. A. Nóbrega and A. Canals, *Anal. Methods*, 2021, **13**, 5670–5678.
9 F. C. Pinheiro, A. I. Barros and J. A. Nóbrega, *Anal. Chim. Acta*, 2019, **1065**, 1–11.
10 S. Grassin-Delyle, M. Martin, O. Hamzaoui, E. Lamy, C. Jayle, E. Sage, I. Etting, P. Devillier and J.-C. Alvarez, *Talanta*, 2019, **199**, 228–237.
11 K. Greda, M. Welna and P. Pohl, *Talanta*, 2022, **246**, 123500.

12 S. Millour, L. Noël, A. Kadar, R. Chekri, C. Vastel and T. Guérin, *J. Food Compos. Anal.*, 2011, **24**, 111–120.
13 F. C. Pinheiro, D. V. Babos, A. I. Barros, E. R. Pereira-Filho and J. A. Nóbrega, *J. Pharm. Biomed. Anal.*, 2019, **174**, 471–478.
14 J. Lin, *Rock Miner. Anal.*, 2021, **40**, 512–521.
15 Y. Chen, H. Liu, S. Chen and W. Yin, *Int. J. Green Technol.*, 2022, **24**, 125–127.
16 Y. Yan, *China Meas. Test*, 2021, **47**, 72–76.
17 G. S. Valasques, G. M. P. Santos, A. L. F. Silva, D. M. F. M. Cerqueira, U. L. C. Ferreira, S. N. L. Santos and M. W. A. Bezerra, *Food Chem.*, 2020, **318**, 126473.
18 M. Atasoy, D. Yildiz, İ. Kula and A. İ. Vaizoğullar, *Food Chem.*, 2023, **401**, 134152.
19 L. Ghezzi, D. M. Valerio and R. Petrini, *Anal. Lett.*, 2023, **56**, 1270–1278.
20 E. Akoury, C. Baroud, S. El Kantar, H. Hassan and L. Karam, *Toxicol Rep*, 2022, **9**, 1962–1967.
21 H. Sun, L. Li, L. Zhang, Z. Zhang, W. Hou, Y. Lei and J. Men, *Fine Chem. Intermed.*, 2023, **53**, 92–96.
22 Y. Yang, S. Xia, H. Li and j. Li, *China Meas. Test*, 2022, **48**, 46–50.
23 J. Liu, *Chin. J. Inorg. Anal. Chem.*, 2020, **10**, 32–37.
24 C. Jin, Z. Hong and L. Yu, *Guangzhou Chem. Ind.*, 2016, **44**, 89–92.
25 H. Li, X. Li, M. Li, W. Guo, L. Jin, Z. Zhu, Q. Hou and S. Hu, *Anal. Methods*, 2022, **14**, 2782–2792.
26 W. Ni, H. Zhang, X. Mao, L. Liu, X. Guo, F. Xiao and X. Gao, *Microchem. J.*, 2020, **158**, 105197.
27 W. Ni, H. Zhang, X. Mao, L. Liu and F. Xiao, *Microchem. J.*, 2019, **150**, 104187.
28 O. O. Ilyinichna, L. S. Michailovich, D. A. Sergeevich and E. K. Gennadievna, *J. Anal. At. Spectrom.*, 2020, **35**, 2627–2638.
29 Y. Yang, S. Xia, H. Li and J. Li, *China Meas. Test*, 2022, **48**, 46–50.
30 S. Zhang and M. Zhou, *J. Anal. Methods Chem.*, 2020, **2020**, 8867653.
31 E. I. Muller, C. C. Muller, J. P. Souza, A. L. H. Muller, M. S. P. Enders, M. Doneda, A. C. Frohlich, G. D. Iop and K. F. Anschau, *Microchem. J.*, 2017, **134**, 257–261.
32 E. I. Muller, J. P. Souza, C. C. Muller, A. L. H. Muller, P. A. Mello and C. A. Bizzi, *Talanta*, 2016, **156–157**, 232–238.
33 J. Lee, Y.-S. Park, H.-J. Lee and Y. E. Koo, *Food Chem.*, 2022, **373**, 131483.
34 A. L. H. Muller, J. S. S. Oliveira, P. A. Mello, E. I. Muller and E. M. M. Flores, *Talanta*, 2015, **136**, 161–169.
35 J. Lee, Y.-S. Park and D. Y. Lee, *Lwt*, 2023, **173**, 114351.
36 W. Yang, J. F. Casey and Y. Gao, *Fuel*, 2017, **206**, 64–79.
37 M. F. Gazulla, M. J. Ventura, M. Orduña, M. Rodrigo and A. Torres, *Talanta Open*, 2022, **6**, 100134.
38 F. C. Pinheiro, D. V. Babos and A. I. Barros, *J. Pharm. Biomed. Anal.*, 2019, **174**, 471–478.
39 F. C. Pinheiro, A. I. Barros and J. A. Nobrega, *Anal. Chim. Acta*, 2019, **1065**, 1–11.
40 G. T. Druzian, M. S. Nascimento, R. S. Picoloto, M. F. Mesko, E. M. M. Flores and P. A. Mello, *J. Anal. At. Spectrom.*, 2022, **37**, 1799–1805.
41 M. Liang and H. Liu, *China Pat.*, CN117214280A, Sun Yat-sen University, China, 2023.
42 *China Standard*, GB/T27418—2017, 2017.
43 Q. Zhang, *Science and Technology & Innovation*, 2016, vol. 01, pp. 104–107.

